ChemPubSoc Europe

DOI: 10.1002/chem.201603765

CHEMISTRY
A European Journal
Full Paper

Substituent Effects

Synthesis of 1,2-Dioxetanes as Thermochemiluminescent Labels for Ultrasensitive Bioassays: Rational Prediction of Olefin Photooxygenation Outcome by Using a Chemometric Approach

Luca A. Andronico, Arianna Quintavalla,* Marco Lombardo,* Mara Mirasoli, Massimo Guardigli, Claudio Trombini, and Aldo Roda[a]

Abstract: Great interest in new thermochemiluminescent (TCL) molecules, for example, in bioanalytical assays, has prompted the design and synthesis of a small library of more than 30 olefins to be subjected to photooxygenation, with the aim of obtaining new 1,2-dioxetane-based TCL labels with optimized properties. Fluorine atoms on the acridan system remarkably stabilize 1,2-dioxetanes when they are located in the 3- and/or 6-position (**4h** and **4i**). On the other hand, 2,7-difluorinated acridan dioxetane (**4j**) showed a significantly enhanced fluorescence quantum yield with respect to the unsubstituted dioxetane (**4a**). Some of the synthesized olefins did not undergo singlet oxygen addition and a rationale was sought to ease the photooxygenation step, leading to the TCL dioxetanes. A chemometric approach has been adopted to exploit principal component analysis and linear discriminant analysis of the structural and electronic molecular descriptors obtained by DFT optimizations of olefins **3**. This approach allows the steric and electronic parameters that govern dioxetane formation to be revealed.

Introduction

From the 1970s to date, the 1,2-dioxetane system[1] has continued to attract great interest due to its key role in chemiluminescence[2] (CL) and bioluminescence[3] (BL) reactions. Its peculiar properties have stimulated and enabled the development of a wide array of applications. For example, recently, 1,2-dioxetanes have been exploited as luminescent mechanophores, namely, responsive units able to transduce mechanical stress into an optical response.[4] Primarily, dioxetane analogues have proved to be potent tools in clinical diagnostics as chemiluminescent substrates for enzymes, such as alkaline phosphatase, used as labels in immunoassays and gene assays.[5] Indeed, CL,[6] BL,[7] and electrogenerated chemiluminescence (ECL)[8] detection techniques are particularly well suited in applications in which high sensitivity is required, offering high detectability, even in low volumes, a wide linear range of responses, and a high signal to noise ratio. Nevertheless, CL, BL, and ECL detection requires the addition of reagents to induce light emission, thus decreasing assay rapidity and simplicity, which are crucial for on-field biosensor applications. The remarkable advantage of a thermochemiluminescence (TCL) label is that its light emission is simply produced by heating, and nothing else. In fact, the TCL phenomenon originates from heating a suitable thermodynamically relatively unstable molecule, which decomposes to yield a product mainly in the singlet excited state that decays with photon emission (see Scheme 1). Nowadays, TCL[9] offers challenging and unexplored opportunities for the development of reagentless and ultrasensitive detection methods exploitable, for example, in simple portable biosensors with TCL molecules as labels, as either single molecules or included in functionalized silica nanoparticles (SiNPs).[10a,b]

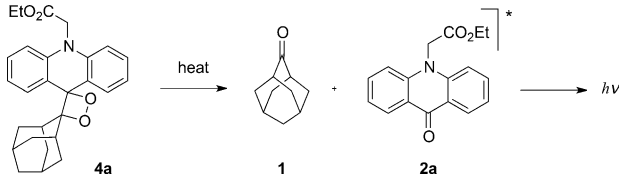

Scheme 1. Acridan-containing 1,2-dioxetane **4a**, which was employed by us as a TCL label.

Thermochemiluminescent 1,2-dioxetanes, described for the first time in 1963, were proposed for analytical applications in the late 1980s with limited success due to the relatively high temperature of decomposition and very poor light emission efficiency.[11] Over the last four years, we have reinvestigated acridan-based 1,2-dioxetanes (for example **4a**;[12] Scheme 1) as TCL compounds. As an application, we incorporated **4a** into SiNPs

[a] L. A. Andronico, Dr. A. Quintavalla, Prof. M. Lombardo, Prof. M. Mirasoli, Prof. M. Guardigli, Prof. C. Trombini, Prof. A. Roda
Department of Chemistry "G. Ciamician"
Alma Mater Studiorum, University of Bologna
Via Selmi 2, 40126 Bologna (Italy)
E-mail: arianna.quintavalla@unibo.it
marco.lombardo@unibo.it

Supporting information for this article is available on the WWW under http://dx.doi.org/10.1002/chem.201603765.

with the aim of generating TCL probes for ultrasensitive immunoassays.[10] SiNPs doped with our acridan-based 1,2-dioxetane displayed remarkable advantages, compared to TCL labels proposed in the past,[11] such as a lower trigger temperature (below 100 °C) and highly improved detectability, comparable with that obtained with enzyme-based CL detection.

In a preliminary stage, we studied the effect of weak electron-donating groups (EDGs), such as methyl substituents, on the acridan moiety of **4a** (**4b**–**4g**; Figure 1).[10c] For example, we found that, with acridones as the emitting species, tri- and tetramethyl-substituted acridones showed the highest fluorescence quantum yields (ϕ_F), in the range of 0.48–0.52. Accordingly, the corresponding 1,2-dioxetanes **4f** and **4g** (Figure 1) presented limit of detection (LOD) values more than one order of magnitude lower than that of the unsubstituted derivative **4a**, as determined by TCL imaging experiments. Moreover, we noticed that the impact of the substituent was greater in the 2-position (and/or 7-position). Methyl groups also caused a clear decrease in the activation energy (E_a) of the thermochemiluminescent reaction. Lastly, we observed that the rate of 1,2-dioxetane formation through photooxygenation of the corresponding alkene strongly depended on the substitution pattern of the acridan moiety.

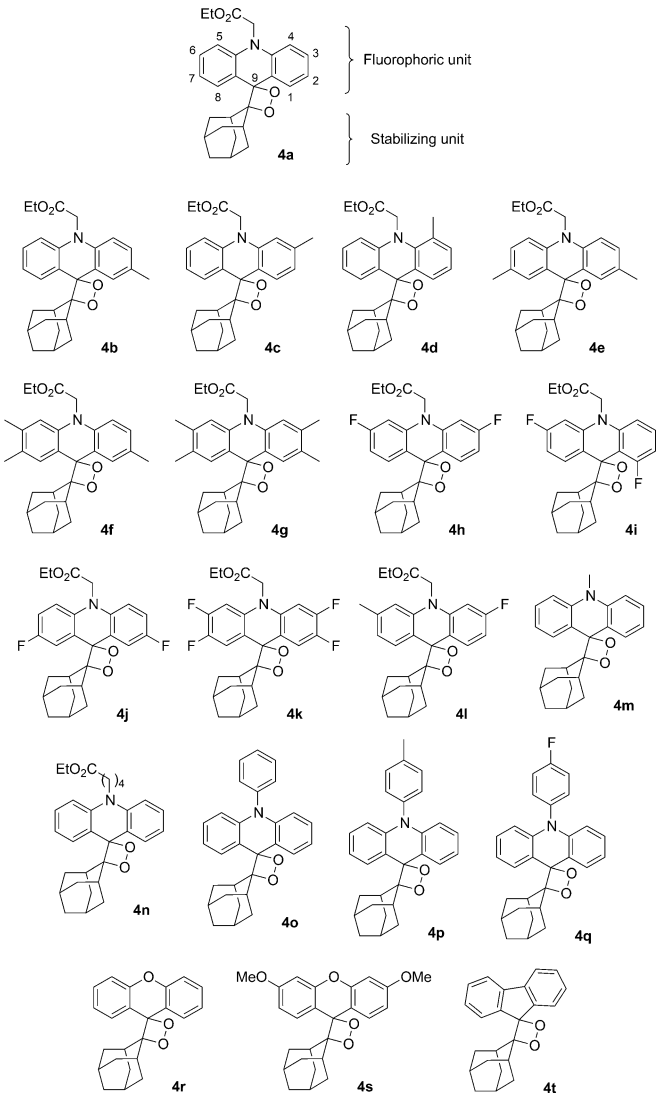

Figure 1. Library of 1,2-dioxetanes studied herein.

Intrigued by the considerable effects of the acridan substituents on the properties of thermochemiluminescent 1,2-dioxetanes, we planned substantial structural modifications to the fluorophore moiety of the dioxetane with the purpose of 1) improving and modulating the photophysical characteristics and activation parameters of the TCL labels, and 2) studying the impact of several structural features on a series of properties of the 1,2-dioxetanes, including the photooxygenation rate of the parent olefin with singlet oxygen ($^1O_2$). The complete list of thermochemiluminescent 1,2-dioxetanes synthesized and investigated is shown in Figure 1. All members of this library were fully characterized in terms of TCL properties.

The synthetic approach to thermochemiluminescent 1,2-dioxetanes **4** is depicted in Scheme 2. It consisted of two steps: a) reductive coupling of two properly selected ketones (**1** and **2**) under McMurry conditions,[13] and b) photooxygenation[14] of the obtained tetrasubstituted alkene **3** to provide the desired 1,2-dioxetane **4**.

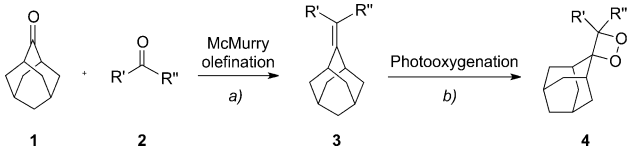

Scheme 2. Two-step synthetic approach to TCL 1,2-dioxetanes **4**.

In a number of cases examined, however, photooxygenation did not occur. Thus, we decided to perform a chemometric investigation with the aim of correlating selected representative structural and electronic features of the olefin reagent with the success of the photooxygenation reaction.

Results and Discussion

Synthesis

At the outset of this study, we optimized the reaction conditions of the two key steps that led to parent 1,2-dioxetane **4a**,[10,12] which was selected as a model compound (see Table S1 in the Supporting Information). The optimized procedure is detailed in Table 1. The most relevant modifications concerning the photooxygenation step were the replacement of polymer-bound Bengal Rose with Methylene Blue as the sensitizer and an increased temperature; these conditions allowed us to achieve better yields in a shorter time.

By using the optimized synthetic protocol, we accomplished a series of modifications on the fluorophoric moiety of **4a** (Table 1), preserving unaltered the adamantyl unit that acts as a stabilizing framework.[15]

Three different structural modifications were examined on parent molecule **4a**. First, we decorated the acridone ring with fluorine substituents, as electron-withdrawing groups (EWGs),

Table 1. Synthesis of differently substituted 1,2-dioxetanes **4a**, **4h–t**.[a]

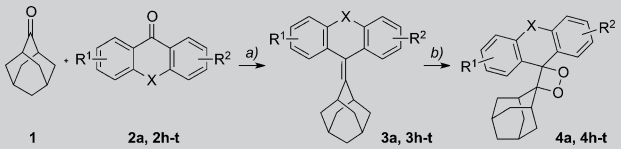

Entry	Ketone **2**	Olefin **3** (yield [%])[b]	1,2-Dioxetane **4** (time [h], yield [%])[b]
1	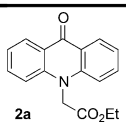 **2a**	**3a** (94)	**4a** (2, 92)
2	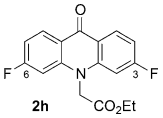 **2h**	**3h** (86)[c]	**4h** (2, 95)
3	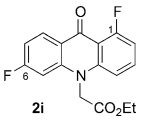 **2i**	**3i** (88)	**4i** (7, 55)[d]
4	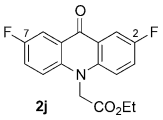 **2j**	**3j** (76)	**4j** (4, 89)
5	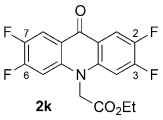 **2k**	**3k** (48)[e]	**4k** (4, 89)
6	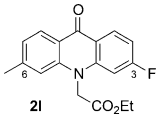 **2l**	**3l** (89)	**4l** (2, 80)
7	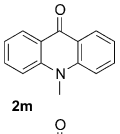 **2m**	**3m** (95)[c]	**4m** (12, 80)[f]
8	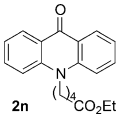 **2n**	**3n** (95)	**4n** (2, 91)[f]
9	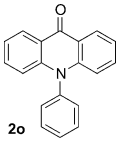 **2o**	**3o** (92)[c]	**4o** (2, 85)
10	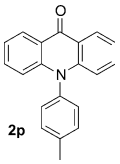 **2p**	**3p** (93)[c]	**4p** (2, 87)[f]
11	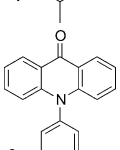 **2q**	**3q** (91)[c]	**4q** (2, 92)
12	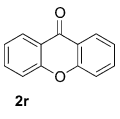 **2r**	**3r** (90)	**4r** (5, 91)

Table 1. (Continued)

Entry	Ketone **2**	Olefin **3** (yield [%])[b]	1,2-Dioxetane **4** (time [h], yield [%])[b]
13	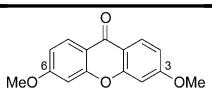 **2s**	**3s** (77)	**4s** (7, 82)[f]
14	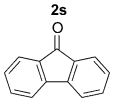 **2t**	**3t** (58)	**4t** (10, 50)

[a] Reaction conditions: a) McMurry coupling: adamantanone **1** (0.28 mmol), ketone **2** (1 equiv), $TiCl_4$ (6.1 equiv), Zn (13.5 equiv), THF (6 mL), reflux, 45 min; b) photooxygenation: Methylene Blue (6.5 mol%), UV cutoff filter ($\lambda = 550$ nm), $-20\,^{\circ}C$, CH_2Cl_2 (1 mL for 10 mg of olefin **3**), 500 W halogen lamp, O_2 (1 atm, balloon). [b] Determined after purification by flash chromatography. [c] Ketone **2** (3.2 equiv), 1.5 h. [d] $-30\,^{\circ}C$. [e] Poor solubility of the starting ketone **2k**. [f] $-40\,^{\circ}C$.

to obtain difluoro- or tetrafluoroacridan derivatives, as well as products containing both fluorine and a methyl substituent as EDG. McMurry olefination proceeded smoothly on acridones **2h–l**, regardless of the substitution pattern, to provide the corresponding alkenes **3h–l** in high yields (up to 89%).

Also, the photooxygenation step provided, in most cases, good results, but the reactivity of various olefins showed some differences. First, we observed that the formal [2+2] cycloaddition of singlet oxygen to acridane-derived alkenes strongly depended on steric hindrance. In fact, when a fluorine atom occupied the 1-position on the aromatic system (Table 1, entry 3), the reaction was significantly slower. On the other hand, the presence of EWGs (two or four fluorine atoms; Table 1, entries 2–4 and 5, respectively) or a combination of an EWG and an EDG (Table 1, entry 6) did not affect 1,2-dioxetane formation.

In the second stage, we replaced the ethyl acetate on the nitrogen with alkyl or aryl substituents (Table 1, entries 7–11). The corresponding 1,2-dioxetanes **4m–q** were always accessible, but when the electron-donating effect was more pronounced (Table 1, entries 7, 8, and 10) we were forced to decrease the photooxygenation temperature to $-40\,^{\circ}C$ to obtain good results, since at $-20\,^{\circ}C$ partial degradation of the dioxetane **4** to the corresponding ketones **1** and **2** occurred.

We also focused our attention on the nature of the endocyclic heteroatom and replaced the nitrogen atom with oxygen (Table 1, entries 12 and 13). The oxygen-bearing xanthyl derivatives **2r** and **2s** smoothly underwent McMurry olefination (**3r,s**) and subsequent photooxygenation; this allowed us to isolate the corresponding 1,2-dioxetanes **4r** and **4s** in high yields after chromatographic purification.[16] The reaction with singlet oxygen was also acceptable (Table 1, entry 14) when a direct linkage between the two aromatic rings was created, as in fluorenone-derived olefin **3t**.[17]

Photophysical and TCL properties

The TCL properties of this series of 1,2-dioxetanes **4h–t** were investigated (Table 2), together with the photophysical properties of the corresponding ketones **2h–t**, which were the emitting species in the TCL process (Scheme 1).[18] For comparison, we also show data for previously reported 1,2-dioxetane **4a** and acridone **2a** (Table 2, entry 1).[10]

When we measured the fluorescence quantum yields (ϕ_F) of ketones **2a** and **2h–t** (Table 2), it appeared clear that the emission performances of the acridones (Table 2, entries 1–11) were strongly affected by the substitution pattern. In particular, compared to reference compound **2a** (Table 2, entry 1), fluorine atoms on the acridone aromatic rings significantly decreased the ϕ_F values when present in the 3- and/or 6-positions (Table 2, entry 2) or in the 1-position (Table 2, entry 3). Conversely, the insertion of fluorines in 2,7-positions enhanced the fluorescence quantum yield (**2j** cf. **2a**, **2k** cf. **2h**). These unexpected and intriguing results suggested that the emitting performances of F-substituted acridane-based ketones were mostly affected by the position rather than the electronic features of the substituents on the aromatic rings. As a further confirmation, by replacing a fluorine atom (EWG) in the 6-position with a methyl group (weak EDG), we obtained only a slight increase in the ϕ_F value (**2l**, entry 6, cf. **2h**, entry 2, Table 2).[19] The observed behavior also proved to be peculiar in comparison with the fluorescence quantum yield trend previously recorded for (poly)methylated acridones.[10c] In the presence of EDGs, the ϕ_F values showed an increase for substitution at both the 2- and 3-positions. On the contrary, the insertion of fluorine atoms generated the opposite effect, depending on their location on the aromatic system.[21] To the best of our knowledge, very few examples are present in the literature that describe the behavior of EWG-substituted 1,2-dioxetanes,[22] and no studies have been reported on fluorine-bearing aryl dioxetanes or concerning the dependence of 1,2-dioxetanes properties on the EWG distribution on the acridan system. In particular, opposite effects on fluorescence quantum yield as a function of the substituent position have never been observed.

After examining the photophysical properties of ketones **2h–l**, we turned our attention to the activation parameters of the thermal decomposition of the fluorinated 1,2-dioxetanes **4h–l**.[23] The trend shown by acridane 1,2-dioxetanes containing EDGs consists of lowered activation energies (E_a) and pre-

Table 2. Photophysical properties of ketones **2a** and **2h–t** and activation parameters for the thermal decomposition of the corresponding 1,2-dioxetanes **4a** and **4h–t**.

Entry	2	ϕ_F[a]	4	E_a [kcal mol^{-1}][b]	ln A [s^{-1}][b]	$t_{1/2}$ [months][c]
1	**2a**	0.11	**4a**	31.5 ± 0.8	35.6 ± 1.0	11
2	**2h**	0.01	**4h**	41.7 ± 4.4	48.0 ± 5.6	1400 (117 years)
3	**2i**	4×10^{-3}	**4i**	36.1 ± 4.3	41.8 ± 5.6	55
4	**2j**	0.65	**4j**	27.9 ± 1.2	30.6 ± 1.5	3.9
5	**2k**	0.11	**4k**	25.8 ± 1.1	28.6 ± 1.4	1.0
6	**2l**	0.04	**4l**	35.1 ± 2.7	42.9 ± 3.5	3.4
7	**2m**	0.61	**4m**	30.9 ± 1.5	37.3 ± 2.0	0.76
8	**2n**	0.44	**4n**	23.7 ± 1.6	27.2 ± 2.2	0.097
9	**2o**	0.28	**4o**	27.7 ± 0.7	31.0 ± 0.9	1.9
10	**2p**	0.43	**4p**	26.2 ± 2.4	29.5 ± 3.3	0.66
11	**2q**	4×10^{-4}	**4q**	32.0 ± 1.4	37.4 ± 1.9	4.4
12	**2r**	1×10^{-4}	**4r**	46.4 ± 3.4	58.0 ± 4.7	180 (15 years)
13	**2s**	2×10^{-4}	**4s**	27.0 ± 1.1	29.5 ± 1.5	2.6
14	**2t**	0.025	**4t**	33.8 ± 1.4	40.8 ± 1.9	3.1

[a] Determined in acetonitrile by using quinine sulfate as standard ($\phi_F = 0.53$ in H_2SO_4 0.05 mol L^{-1}). [b] Mean ± SD of three independent measurements. [c] Calculated for the solid compound at 25 °C.[20]

exponential coefficients (A) and increased fluorescence quantum yields (ϕ_F).[10c] We reasoned that the introduction of fluorine atoms as EWGs should give more stable and easy to handle 1,2-dioxetanes, without causing an excessive impairment of the fluorescence quantum yield. The activation parameters recorded for the fluorinated 1,2-dioxetanes confirmed our hypothesis, but they also revealed some unexpected results. The 3,6-difluorodioxetane **4h** (Table 2, entry 2) was characterized by the highest activation energy ($E_a = 41.7$ kcal mol^{-1}) and showed an outstanding and unprecedented calculated half-life ($t_{1/2}$) of 117 years, if stored as a solid at 25 °C.[24] Increased stability compared with unsubstituted dioxetane **4a** was also recorded for compound **4i** (Table 2, entry 3; $E_a =$ 36.1 kcal mol^{-1}, $t_{1/2} = 55$ months), whereas the remaining fluorinated dioxetanes **4j–l** (Table 2, entries 4–6) proved to be less thermally stable. The results obtained from this family of compounds confirmed that there was a correlation between acridone fluorescence quantum yield and thermal stability of the corresponding 1,2-dioxetane. The substituents on the aromatic system that enhance the ϕ_F value, such as fluorine atoms in the 2,7-positions (**2j–k**), facilitate dioxetane thermal decomposition (**4j–k**) at the same time. Conversely, 3,6-difluoro- (**2h**) and 1,6-difluoro-substituted (**2i**) acridones showed decreased fluorescence quantum yields, but the corresponding dioxetanes **4h–i** displayed significantly longer half-life values. A comparison of these data with those recorded for methyl-substituted acridan-based dioxetanes[10c] confirmed that the introduction of weak EDGs increased the ketone fluorescence quantum yield[25] and lowered the dioxetane activation energy, regardless of the position on the aromatic ring. On the contrary, the impact of fluorine atoms depended dramatically on the substituent position.

The second structural feature we studied was the nature of the substituent on the acridan nitrogen (Table 2, entries 7–11).[26] Removing (**2m**, **4m**) or elongating (**2n**, **4n**) the ester group present in the parent compounds (**2a**, **4a**) provided the expected enhancement of ϕ_F and decrease in E_a values (Table 2, entries 7 and 8, respectively). This finding further confirmed the stabilizing effect postulated for the acetate moiety, due to its electron-withdrawing character.[10d,12a] Then, we investigated *N*-aryl derivatives (**2o–q**, **4o–q**; Table 2, entries 9–11) and observed, in general, a lower thermal stability of the dioxetanes[27] with respect to the reference compound **4a**, even if the decrease was more pronounced for the EDG-substituted compound **4p** than that for the *para*-fluorophenyl derivative **4q**.

Thus, for acridane-based 1,2-dioxetanes, we conclude that 1) the introduction of fluorine atoms onto the aromatic rings represents a remarkable tool to stabilize the dioxetane derivatives, in particular, when they are located at the 3- and/or 6-position, or to enhance their emitting performances, when located at the 2,7-positions; 2) the acetate moiety proves to be the best performing *N*-substituent, ensuring a good balance between ketone fluorescence quantum yield and dioxetane stability.

As far as the activation parameters for the thermal decomposition of xanthyl-derived 1,2-dioxetanes (**4r,s**) and the photophysical properties of the corresponding emitting species **2r** and **2s** are concerned, we observed that the replacement of the endocyclic nitrogen with an oxygen provided a very stable dioxetane (**4r**), but also strongly decreased the fluorescence quantum yield (cf. Table 2, entries 1 and 12). Moreover, EDGs on the xanthyl scaffold (3,6-positions) dramatically decreased the activation parameters without a perceptible benefit in the ϕ_F value (cf. Table 2, entries 12 and 13). Lastly, fluorenyl dioxetane **4t**, which featured a direct linkage between the aromatic rings, afforded acceptable emitting properties ($\phi_F = 0.025$) accompanied by moderate thermal stability (Table 2, entry 14).

Chemometric analyses

To widen our library of TCL 1,2-dioxetanes and to learn more about the structure–property relationships of this class of com-

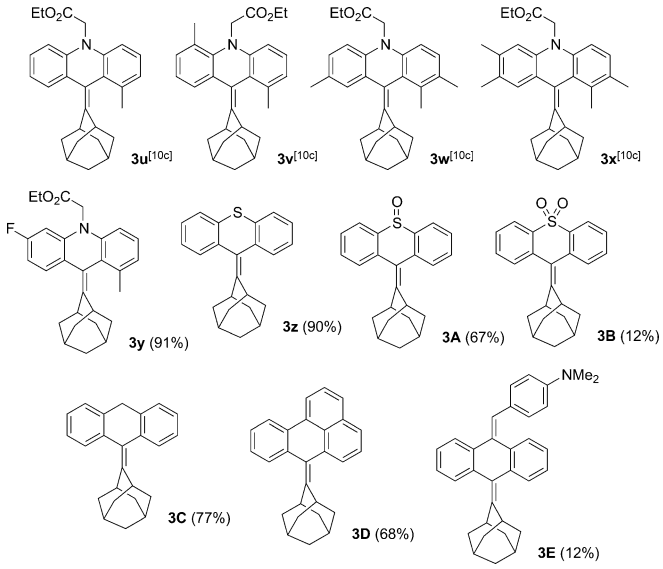

Figure 2. Differently substituted alkenes unreactive under photooxygenation conditions (the yields of olefin formation are given in parentheses; for synthetic details, see the Supporting Information).

pounds, we also synthesized a series of olefins that, unexpectedly, did not undergo the photooxygenation step (Figure 2).

Previously investigated acridane-based alkenes **3u**–**x**[10c] and the 1-Me, 6-F derivative **3y** are all characterized by the presence of a methyl group at the 1-position of the aromatic system. Such results suggest that steric crowding in this region disfavors the addition of singlet oxygen. The slow photooxygenation rate observed for 1,6-difluoro compound **3i** (Table 1, entry 3) supports this hypothesis.

The sulfur-containing olefins **3z**–**B** did not react with singlet oxygen, regardless of the sulfur oxidation state.[28] We tested other reaction temperatures (namely, 0 and −20 °C) and extended the reaction times up to 7 h, but only the starting olefin was recovered. Finally, when we replaced the endocyclic heteroatom with a sp^3- or sp^2-hybridized carbon (**3C**–**E**), in all cases, photooxygenation did not occur.

These findings reveal that the reactivity of an olefin in the photooxygenation process strongly depends on its substitution pattern. It is known that the formal [2+2] cycloaddition of singlet oxygen to alkenes takes place efficiently on electron-rich systems.[29] However, the mechanism of this process has been extensively debated in the literature (Scheme 3),[30] and the most reliable one can vary case by case, depending on the molecular structure of the substrate,[30a,d–i,k] the solvation energy,[30a,e,i] and also the sensitizer employed.[30b,c,j,l] As a consequence, the nature of the olefin substituents (electron-donating ability, presence of hydrogen-bond acceptors and/or donors, geometry, and steric hindrance) not only affects the success of singlet oxygen addition, but it also determines the reaction pathway.

The mechanism of singlet oxygen addition to double bonds has been studied computationally several times, but the rigorous approach to this diradical system requires expensive treatments of multireference states and it has been applied exclu-

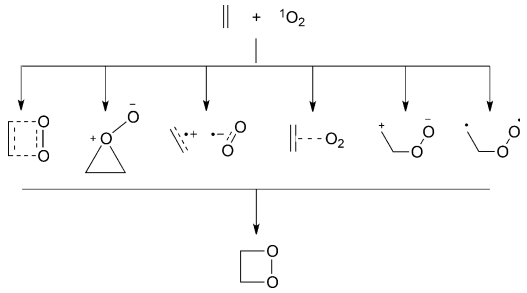

Scheme 3. A representation of the various hypothesized mechanisms for the formation of 1,2-dioxetanes through singlet oxygen addition to olefins.

sively on very simple systems.[31] Moreover, the prediction of the mechanism of singlet oxygen reactions has proven a challenging task for many reasons,[32] including because different possible reaction pathways (Scheme 3) are often predicted depending on the level of theory employed.[33]

To rationalize all of our results, we decided to avoid an extremely demanding and time-consuming quantum mechanical approach, considering that both excited and radical states are involved in the reaction. Rather, we envisioned a chemometric approach as a more practical tool to identify which structural and electronic properties of starting olefins, or combination of them, determine the success of the photooxygenation step.

At the outset, we adopted principal component analysis (PCA)[34] of the structural and electronic molecular descriptors obtained by DFT optimizations of olefins **3**.[35] After an initial conformational screening by using a molecular mechanics (MM) force field on the data set of molecules, the conformers obtained in a 8 kcal mol^{-1} window were optimized by using DFT at the B3LYP/6-31G(d) level of theory (see the Supporting Information for details). Among the different calculated electronic descriptors, we selected the energy of the HOMO, the energy of the LUMO, the Mulliken charges on the olefin carbon terminals Ca-Mul and C9-Mul (Figure 3) and the coefficients of the atomic contribution of the alkene carbon atoms to the HOMO and LUMO orbitals, calculated by using the Mulliken decomposition method (Ca-HOMO, Ca-LUMO, C9-HOMO, and C9-LUMO). Moreover, we selected a few structural parameters that reflect the geometry of the molecules in close proximity to the double-bond reaction site. In particular, we chose

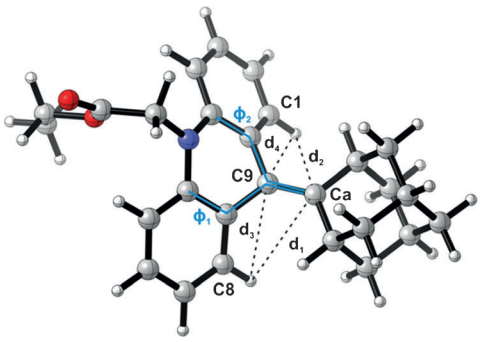

Figure 3. DFT-optimized structure of **3a** and structural molecular descriptors employed in the PCA.

the two dihedral angles, ϕ_1 and ϕ_2, which represent the deviation from planarity of the aromatic rings with respect to the plane defined by the carbon–carbon double bond, and the four interatomic distances d_1–d_4 as an index of steric crowding of the aromatic ring substituents around the Ca–C9 double bond (Figure 3). Specifically, when a substituent was present in the C1 position of the aromatic system, d_2 and d_4 were taken as the interatomic distances between the double-bond carbon atoms Ca and C9 and the closest atom of the substituent group, as shown in Figure 3.

We analyzed first a set of 23 similar molecules that possessed a common acridane skeleton (**3a–q**, **3u–y**, and **3F**; Figure 4),[10c,12d] the molecular descriptors of which are collected

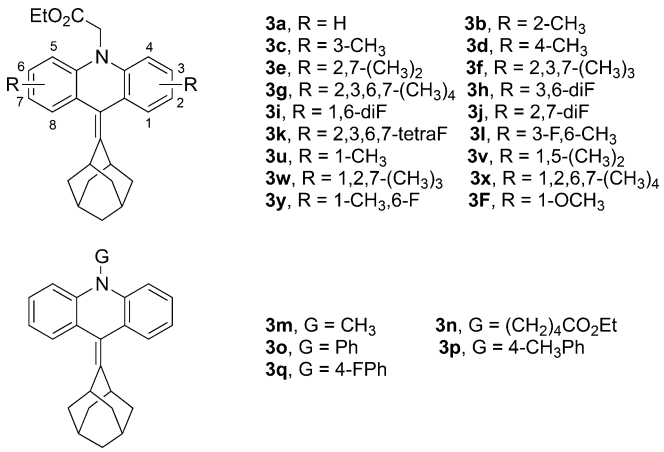

3a, R = H; **3b**, R = 2-CH_3; **3c**, R = 3-CH_3; **3d**, R = 4-CH_3; **3e**, R = 2,7-$(CH_3)_2$; **3f**, R = 2,3,7-$(CH_3)_3$; **3g**, R = 2,3,6,7-$(CH_3)_4$; **3h**, R = 3,6-diF; **3i**, R = 1,6-diF; **3j**, R = 2,7-diF; **3k**, R = 2,3,6,7-tetraF; **3l**, R = 3-F,6-CH_3; **3u**, R = 1-CH_3; **3v**, R = 1,5-$(CH_3)_2$; **3w**, R = 1,2,7-$(CH_3)_3$; **3x**, R = 1,2,6,7-$(CH_3)_4$; **3y**, R = 1-CH_3,6-F; **3F**, R = 1-OCH_3

3m, G = CH_3; **3n**, G = $(CH_2)_4CO_2Et$; **3o**, G = Ph; **3p**, G = 4-CH_3Ph; **3q**, G = 4-FPh

Figure 4. Initial set of acridan-containing alkenes analyzed with the chemometric approach.

in Table S3 in the Supporting Information. Data were mean-centered before analysis and were autoscaled by dividing them by the standard deviation of each column sample variable. The first four eigenvalues greater than 1 obtained by PCA of the 23×14 data matrix and the explained variances relative to each component are reported in Table 3. The model obtained is able to explain 84.9% of the total variance by using only three PCs, whereas two PCs explain 64.7% of the variance.

The score plot representing the projections of the data points in the plane defined by the two first PCs is reported in Figure 5A. A clustering of data is apparent, with the alkenes that undergo photooxygenation grouped in the right side of the plot (blue triangles) and the unreactive molecules clustered on the left (red dots), mainly discriminated by the first PC.

The loading plot, reported in Figure 5B with the variables colored by relative contributions, shows that the variables mainly composing the first PC are the Mulliken charge C9-Mul ($\cos^2=0.834$), the dihedral angles ϕ_1 and ϕ_2 ($\cos^2=0.808$ and 0.807, respectively), the interatomic distances d_2 and d_4 ($\cos^2=$ 0.815 and 0.669, respectively), and, to a lesser extent, the interatomic distance d_1 ($\cos^2=0.541$) and the Mulliken charge Ca-Mul ($\cos^2=0.582$). The only variables significantly contributing to the second PC are the interatomic distance d_3 ($\cos^2=$ 0.641) and, to a lesser extent, the interatomic distance d_1 ($\cos^2=0.413$) and the energies of the HOMO and LUMO orbitals ($\cos^2=0.461$ and 0.483, respectively). PCA results seem to suggest that the difference in reactivity in the photooxygenation reaction between the two groups of alkenes is mainly due to steric effects and not to electronic ones. In particular, the presence of a bulky methyl group in the 1-position of the acridan skeleton results in a significantly larger deviation from planarity for compounds **3u–y**, with respect to all other reactive alkenes (see Table S3 in the Supporting Information). This geometrical distortion has the overall effect of making the Ca–C9 double bond more sterically crowded and less accessible to singlet oxygen, as also evidenced by the shorter interatomic distances d_1 and d_2 in the unreactive compounds.

The same analysis was repeated on the expanded data set comprising the oxygen-bearing xanthyl derivatives **3r–s** (**XAN** family), the sulfur-containing olefins **3z**, **3A**, and **3B** (**THI** family), and the anthrone-derived alkenes **3C–E** (**ANT** family), in addition to the previously analyzed acridane derivatives **3a–q**, **3u–y**, and **3F** (**ACR** family). The eigenvalues greater than 1 derived from PCA of the as-obtained 31×14 data matrix are reported in Table 4, while the corresponding molecular descriptors employed are collected in Table S4 in the Supporting Information. By using the first three PCs, the model can be used to explain 73.8% of the total variance, whereas 56% of the variance is accounted for by using only the first two PCs.

The score plot representing the projections of the data points in the plane defined by the two first PCs is reported in Figure 6A and the corresponding loading plot with the variables colored by relative contributions is shown in Figure 6B.

Again, a quite marked separation in the score plot is apparent between the reactive and unreactive olefins, which in this expanded data set is discriminated by both the first and second PCs.

Table 3. Eigenvalues and percentage of explained variance relative to the first four principal components (PCs) of the model used for the description of olefins **3a–q**, **3u–y**, and **3F**.

PC	Eigenvalue	Variance [%]	Cumulative Eigenvalue	Cumulative variance [%]
PC1	5.96	42.5	5.96	42.5
PC2	3.11	22.2	9.07	64.7
PC3	2.82	20.1	11.89	84.9
PC4	1.16	8.3	13.05	93.1

Table 4. Eigenvalues and percentage of explained variance relative to the first five PCs of the model used for the description of olefins **3a–s**, **3u–z**, and **3A–F**.

PC	Eigenvalue	Variance [%]	Cumulative Eigenvalue	Cumulative variance [%]
PC1	4.45	31.8	4.45	31.8
PC2	3.39	24.2	7.84	56.0
PC3	2.49	17.8	10.33	73.8
PC4	1.42	10.1	11.75	83.9
PC5	1.09	7.8	12.84	91.6

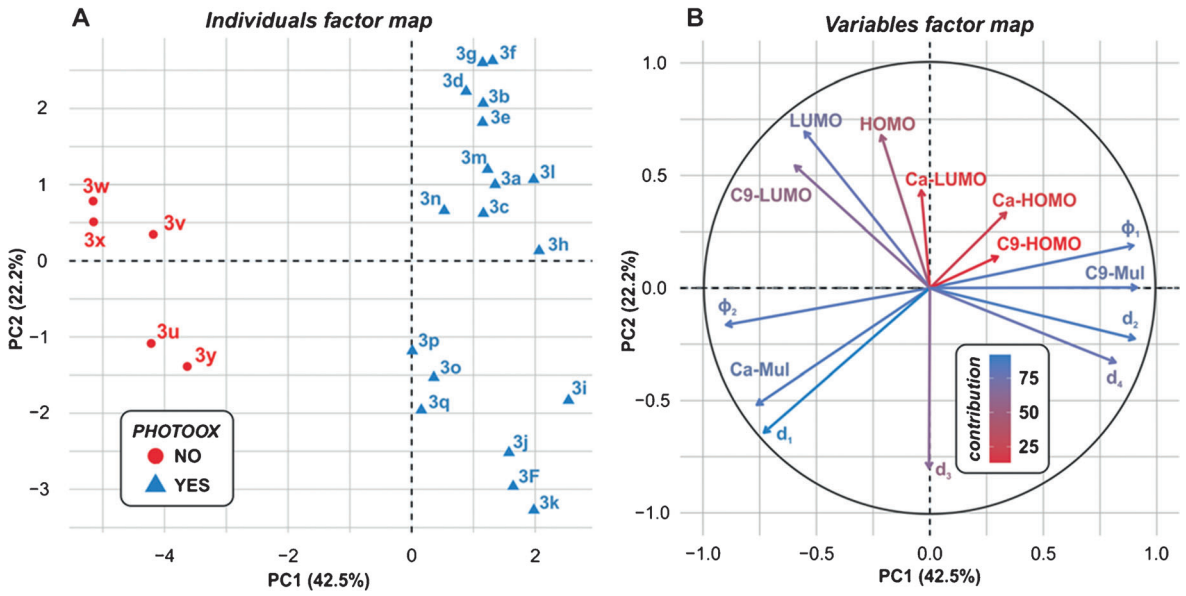

Figure 5. PCA results for the data matrix descriptors of olefins **3a–q**, **3u–y**, and **3F**: A) PCA score plot relative to the first two PCs (blue triangles: reactive compounds; red dots: unreactive compounds). B) PCA loading plot relative to the first two PCs (variables are colored according to their relative contribution).

The relative loading plot (Figure 6B) reveals that the variables contributing to the first PC are mainly the steric parameters, similarly to what is obtained for the previously analyzed **ACR** family. In particular, the highest contributing variables are mainly the dihedral angles ϕ_1 and ϕ_2 ($\cos^2 = 0.906$ and 0.915, respectively) and, to a lesser extent, the interatomic distances d_2 and d_4 ($\cos^2 = 0.632$ and 0.542, respectively) and the Mulliken charge Ca-Mul ($\cos^2 = 0.654$). On the other hand, the variables significantly contributing to the second PC are mainly electronic parameters, namely, the energies of the HOMO and LUMO ($\cos^2 = 0.592$ and 0.759, respectively) and, to a lesser extent, the Mulliken charge C9-Mul ($\cos^2 = 0.475$).

For this expanded data set, the PCA results suggest that both steric and electronic effects play a role in determining the reactivity under photooxygenation conditions; both factors are necessary, but not sufficient to trigger reactivity. The score plot of the data projections (Figure 6A) is apparently divided into four quadrants, with the reactive olefins in the top-right sector, where both steric and electronic parameters cooperate in the same positive direction. The acridane-containing unreactive olefins (**3u–y**) are positioned in the top-left quadrant, in a region where electronic effects alone would allow the photooxygention reaction, which is hampered solely by steric hindrance around the Ca–C9 double bond exerted by the methyl

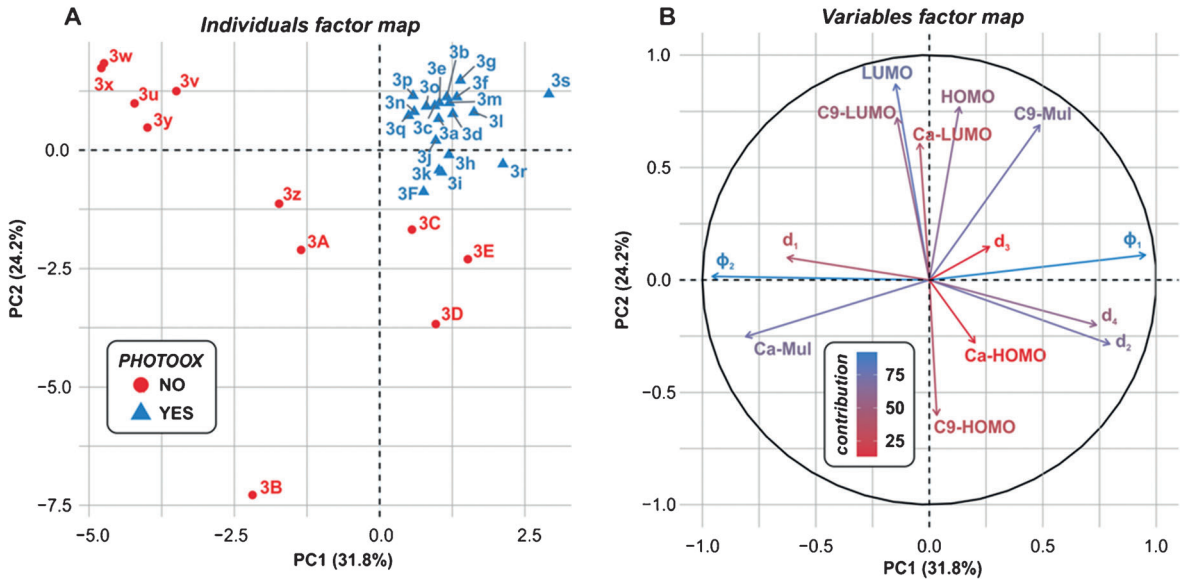

Figure 6. PCA results for the data matrix descriptors of olefins **3a–s**, **3u–z**, and **3A–F**: A) PCA score plot relative to the first two PCs (blue triangles: reactive compounds; red dots: unreactive compounds); B) PCA loading plot relative to the first two PCs (variables are colored according to their relative contribution).

group present at the 1-position (121–124° versus 130° mean ϕ_1/ϕ_2 values for all compounds). On the other hand, the anthrone-derived alkenes **3C–E** are grouped in the bottom-right sector of the score plot, with the same coordinates of the reactive olefins along the first PC. Although photooxygenation should not be disallowed for steric reasons for these alkenes, the overall linear combination of their electronic descriptors renders them unreactive. The sulfur-containing olefins **3z** and **3A** are located in a borderline central region of the plot, where both steric and electronic factors are not ideal for promoting the photooxygention reaction, whereas the sulfone analogue **3B** is projected farther away along the negative PC2 axis. Finally, the reactive xanthyl derivatives **3r** and **3s** are correctly projected in the same top-right quadrant of the previously examined reactive acridane-based olefins, which possess both steric and electronic properties that allow the photooxygenation reaction to proceed smoothly. The score plot of the expanded data set relative to the first two PCs is again reported in Figure 7, with the projected data points now colored according to the common structural features of the employed alkenes (**XAN**: **3r,s**; **THI**: **3z**, **3A,B**; **ANT**: **3C–E**, and **ACR**: **3a–q**, **3u–y**, **3F**). The marked clustering obtained in this plot clearly shows the capability of the PCA model to discriminate between different alkenes on the basis of their common structural features.

To further validate our chemometric approach, a supervised linear discriminant analysis (LDA)[34c,d] was performed on the expanded 31×14 data set. Using the previously chosen parameters, we obtained a highly statistically significant model (Wilks' lambda = 0.0121, canonical correlation = 0.9939), showing perfect discrimination between the two classes of reactive (mean of canonical variables = 6.48) and unreactive olefins (mean of canonical variables = −11.8). The corresponding raw and standardized coefficients of the obtained linear discriminant are reported in Table 5, whereas the canonical scores are plotted in Figure 8 for all compounds.

It is interesting to note that, when LDA was performed by using a stepwise forward variable selection, only 8 of the 14 variables were used to obtain a statistically significant model (Wilks' lambda = 0.0191). Moreover, the most contributing variables were almost exactly the same as those that composed the main PCs of the corresponding PCA, namely, the dihedral angle ϕ_1, the interatomic distances d_2 and d_4, and the Mulliken charges Ca-Mul and C9-Mul.

To verify the capability of the LDA model to predict the reactivity of new compounds with singlet oxygen, the fluorenyl

Table 5. Raw and standardized coefficients of the linear discriminant obtained in the LDA model used for the description of olefins **3a–s**, **3u–z**, and **3A–F**.

Variable	Raw coefficient	Standardized coefficient
HOMO	9.549	3.176
LUMO	−4.564	−1.216
Ca-Mul	865.7	6.167
C9-Mul	83.51	1.631
ϕ_1	0.8260	1.664
ϕ_2	−1.319	−3.620
d_1	−84.28	−2.000
d_2	32.63	2.630
d_3	−3.254	−0.05056
d_4	−6.801	−0.3888
Ca-HOMO	31.76	1.629
C9-HOMO	−40.83	−1.979
Ca-LUMO	23.65	0.7734
C9-LUMO	154.1	2.684
constant	−194.9	–

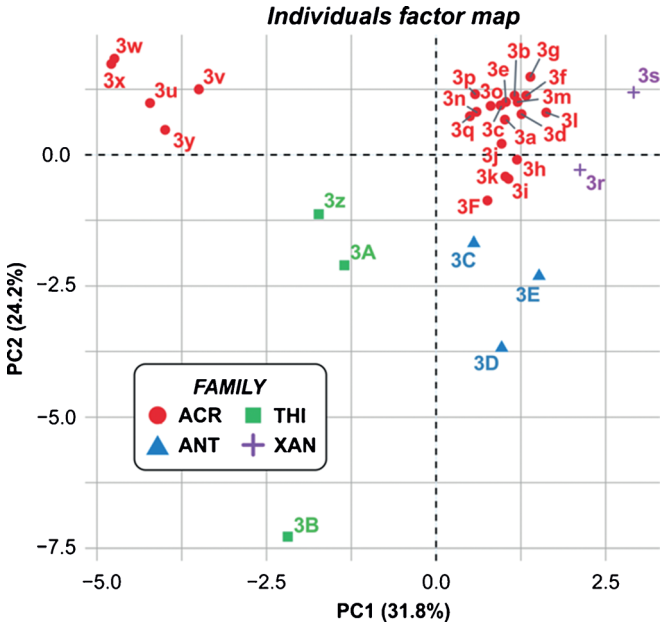

Figure 7. PCA results for the data matrix descriptors of olefins **3a–q**, **3u–y**, and **3F** (**ACR**); **3r-s** (**XAN**); **3z**, **3A–B** (**THI**); and **3C–E** (**ANT**). PCA score plot relative to the first two PCs, colored according to the structural features of the analyzed alkenes.

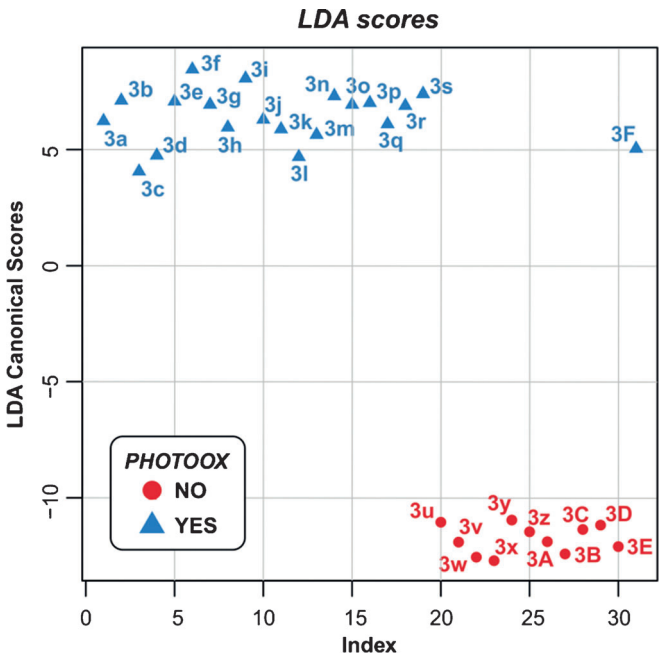

Figure 8. Canonical scores relative to the LDA model for alkenes **3a–s**, **3u–z** and **3A–F**.

alkene **3t** (central five-membered ring) and the specially designed new olefin **3G** (central seven-membered ring; Figure 9) were projected onto the linear discriminant.

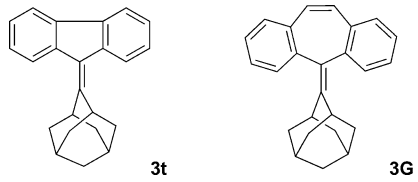

Figure 9. Olefins selected to verify the capability of the model to predict reactivity with singlet oxygen.

The fluorenyl-derived alkene **3t** was predicted to be reactive with a raw canonical score of 30.8; a particularly high value due to an almost completely planar arrangement of the aromatic rings with respect to the plane defined by the carbon–carbon double bond (ϕ_1, $\phi_2 = 159.8^\circ$). As already mentioned in Table 1, entry 14, when **3t** was subjected to the photooxygenation conditions, the corresponding 1,2-dioxetane **4t** was isolated in 50% yield overall. On the contrary, 5-dibenzosuberenone-derived alkene **3G** was predicted to be unreactive with a raw canonical score of −39.9, again a particularly low value, mainly due to its significantly smaller dihedral angles ϕ_1 and ϕ_2 (113.3°) and to the greater negative Mulliken charge on C9 (−0.165 versus −0.09 mean C9-Mul charge). When subjected to the photooxygenation conditions, olefin **3G** did not react and only the starting material was observed in the reaction mixture.

The experimental findings obtained for the supplementary alkenes **3t** and **3G** validate the developed chemometric model, which is able to anticipate the outcome of a photooxygenation reaction carried out on structurally different tetrasubstituted olefins, as characterized by an adamantyl unit coupled to a tricyclic aromatic scaffold (regardless of the nature of the central ring).

Conclusion

A small library of more than 30 olefins of general structure **3** have been subjected to photooxygenation, with the aim of synthesizing new dioxetane-based thermochemiluminescent labels with optimized light emission efficiency and CL temperature triggering. Among them, 20 starting olefins provided the corresponding 1,2-dioxetanes, whereas no traces of product were observed with the other members of the series. To anticipate the feasibility of the photooxygenation step leading to new potentially thermochemiluminescent dioxetanes, we sought a rationale. A complete DFT analysis of the transition states for the formation of all dioxetanes was not possible for us, given the heavy and time-consuming computational effort required by the multiconfigurational treatment of both closed-shell and free-radical excited states at a rigorous level. Thus, we adopted a chemometric approach by exploiting PCA and LDA of the structural and electronic molecular descriptors obtained by DFT optimizations of olefins **3**. This approach allowed us to determine steric and electronic parameters that govern dioxetane formation. Great interest in new thermochemiluminescent molecules, for example, in bioanalytical assays, was the driving force of this study, which allowed us to discover that fluorine atoms on the acridan system remarkably stabilized 1,2-dioxetanes when located in the 3- and/or 6-position (**4h** and **4i**). On the other hand, 2,7-difluorinated acridane dioxetane **4j** showed a significantly enhanced fluorescence quantum yield with respect to the unsubstituted dioxetane **4a**. Our investigations for the development of original and enhanced dioxetane-based TCL labels are still ongoing. For instance, flavone-[36] and coumarin-containing[37] derivatives **4H** and **4I** (Scheme 4) are of interest. Indeed, even if their synthesis still requires some optimization, 1,2-dioxetanes **4H** and **4I** have been isolated and characterized as TCL compounds.

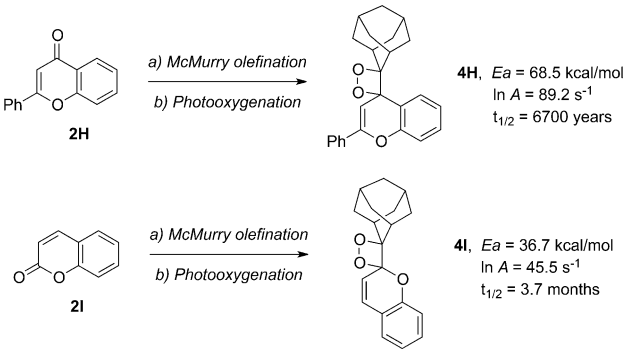

Scheme 4. Preliminary results concerning flavone- (**4H**) and coumarin-based (**4I**) 1,2-dioxetanes.

Unexpectedly high values of the activation parameters for thermal decomposition were recorded for flavone-derived 1,2-dioxetane **4H**, which resulted in a remarkable calculated half-life at 25 °C (more than 6000 years); this offers the opportunity of useful applications in diagnostics and bioanalysis. On the other hand, coumarin-based 1,2-dioxetane **4I** showed limited thermal stability. An analogous chemometric approach will be reported in due course for flavones and coumarins once a significant number of compounds has been synthesized.

Experimental Section

Representative procedure for the synthesis of alkenes 3

Under a nitrogen atmosphere, $TiCl_4$ (1 M in dichloromethane, 6.1 equiv) was added to a suspension of zinc powder (13.5 equiv) in anhydrous THF (8 mL/0.5 mmol of **1**) at 0 °C, and the suspension was stirred for 10 min under reflux. A solution of ketone **2** (1 equiv) and 2-adamantanone **1** (1 equiv) in dry THF (2 mL/0.5 mmol of **1**) was added dropwise over a period of 30 min. The reaction mixture was heated at reflux for 45 min. Then, it was cooled to room temperature, quenched with water, and extracted with AcOEt (3×10 mL). The combined organic layers were dried over sodium sulfate and evaporated under vacuum. The crude product was purified by flash chromatography on silica gel.

Representative procedure for the synthesis of 1,2-dioxetanes 4

Alkene **3** (16 equiv) and Methylene Blue (1 equiv) were dissolved in CH_2Cl_2 (1 mL/10 mg of alkene **3**). The solution was cooled (usually at $-20\,^{\circ}C$) and subjected to an oxygen atmosphere (1 atm, balloon). The solution was stirred at the same temperature under irradiation by using a 500 W halogen lamp equipped with an UV cutoff filter (0.5% transmission at $\lambda = 550$ nm). Irradiation was continued until the starting material disappeared (usually 2 h of irradiation), and the conversion was monitored by ^1H NMR spectroscopy. Product **4** was purified by rapid filtration on a 5 mm layer of silica gel, by using cooled ($-40\,^{\circ}C$) CH_2Cl_2 as the eluent, and the filtered solution was evaporated under vacuum at $0\,^{\circ}C$.

Acknowledgements

Acknowledgement for financial support is made to MIUR (Rome), University of Bologna, and FARB Project (RFBO128121, "Advanced ultrasensitive multiplex diagnostic systems based on luminescence techniques").

Keywords: fluorine · olefination · photooxygenation · substituent effects · thermochemiluminescence

[1] For reviews on 1,2-dioxetanes, see: a) P. D. Bartlett, M. E. Landis, in *Singlet Oxygen*, (Eds.: H. H. Wasserman, R. W. Murray), Academic Press, New York, **1979**, pp. 243 – 286; b) W. Adam, in *The Chemistry of Peroxide*, (Ed.: S. Patai), Wiley, New York, **1983**, pp. 829 – 920; c) W. Adam, in *Small Ring Heterocycles*, (Ed.: A. Hassner), Wiley, New York, **1986**, pp. 351 – 429; d) W. Adam, M. Heil, T. Mosandl, C. R. Saha-Möller, in *Organic Peroxides*, (Ed.: W. Ando), Wiley, New York, **1992**, pp. 221 – 254; e) C. R. Saha-Möller, W. Adam, in *Comprehensive Heterocyclic Chemistry II A Review of the Literature 1982 – 1995*, (Ed.: A. Padwa), Pergamon, New York, **1996**, pp. 1041 – 1082; f) W. Adam, A. V. Trofimov, in *The Chemistry of Peroxides*, (Ed.: Z. Rappoport), Wiley, New York, **2006**, pp. 1171 – 1209.

[2] For reviews on 1,2-dioxetane-based CL, see: a) G. B. Schuster, *Acc. Chem. Res.* **1979**, *12*, 366 – 373; b) M. Matsumoto, *J. Photochem. Photobiol. C* **2004**, *5*, 27 – 53; c) W. J. Baader, C. V. Stevani, E. L. Bastos, in *The Chemistry of Peroxides*, (Ed.: Z. Rappoport), Wiley & Sons, Chichester, **2006**, pp. 1211 – 1278; d) L. F. M. L. Ciscato, D. Weiss, R. Beckert, E. L. Bastos, F. H. Bartoloni, W. J. Baader, *New J. Chem.* **2011**, *35*, 773 – 775; e) A. P. Schaap, S. D. Gagnon, *J. Am. Chem. Soc.* **1982**, *104*, 3504 – 3506; f) M. Matsumoto, N. Watanabe, *Bull. Chem. Soc. Jpn.* **2005**, *78*, 1899 – 1920; g) N. J. Turro, P. Lechtken, N. E. Shore, G. Schuster, H.-C. Steinmetzer, A. Yekta, *Acc. Chem. Res.* **1974**, *7*, 97 – 105.

[3] For information on 1,2-dioxetanes in BL, see: a) E. S. Vysotski, J. Lee, *Acc. Chem. Res.* **2004**, *37*, 405 – 415; b) O. Shimomura, T. Goto, F. H. Johnson, *Proc. Natl. Acad. Sci. USA* **1977**, *74*, 2799 – 2802; c) J.-Y. Koo, S. P. Schmidt, G. B. Schuster, *Proc. Natl. Acad. Sci. USA* **1978**, *75*, 30 – 33.

[4] a) Y. Chen, A. J. H. Spiering, S. Karthikeyan, G. W. M. Peters, E. W. Meijer, R. P. Sijbesma, *Nat. Chem.* **2012**, *4*, 559 – 562; b) Z. S. Kean, J. L. Hawk, S. Lin, X. Zhao, R. P. Sijbesma, S. L. Craig, *Adv. Mater.* **2014**, *26*, 6013 – 6018; c) Y. Chen, R. P. Sijbesma, *Macromolecules* **2014**, *47*, 3797 – 3805.

[5] For chemiluminescent 1,2-dioxetanes as probes for bioanalysis, in particular, CL immunoassays, see: a) A. Mayer, S. Neuenhoefer, *Angew. Chem. Int. Ed. Engl.* **1994**, *33*, 1044 – 1072; *Angew. Chem.* **1994**, *106*, 1097 – 1126; b) W. Adam, D. Reinhardt, C. R. Saha-Möller, *Analyst* **1996**, *121*, 1527 – 1531; c) S. Beck, H. Koster, *Anal. Chem.* **1990**, *62*, 2258 – 2270; d) J. C. Hummelen, T. M. Luider, H. Wynberg, in *Complementary Immunoassays*, (Ed.: W. P. Collins), John Wiley & Sons, Chichester, UK, **1988**; e) T. M. Luider, J. C. Hummelen, J. N. Koek, D. Oudman, H. Wynberg, in *Luminescence Immunoassay and Molecular Applications*, (Ed.: K. Van Dyke), CRC Press, Boca Raton, **1990**; f) I. Bronstein, B. Edwards, J. C. Voyta, *J. Biolumin. Chemilumin.* **1989**, *4*, 99 – 111; g) B. Edwards, A. Sparks, J. C. Voyta, I. Bronstein, *J. Biolumin. Chemilumin.* **1990**, *5*, 1 – 4; h) R. C. Buxton, B. Edwards, R. R. Juo, J. C. Voyta, R. Bethell, *Anal. Biochem.* **2000**, *280*, 291 – 300; i) S. Sabelle, P.-Y. Renard, K. Pecorella, S. de Suzzoni-Dézard, C. Créminon, J. Grassi, C. Mioskowski, *J. Am. Chem. Soc.* **2002**, *124*, 4874 – 4880; j) B. Edwards, A. Sparks, J. C. Voyta, I. Bronstein, in *Bioluminescence and Chemiluminescence, Fundamentals and Applied Aspects*, (Eds.: A. K. Campbell, L. J. Kricka, P. E. Stanley), Wiley, Chichester, **1994**, pp. 56 – 59; k) I. Bronstein, J. C. Voyta, G. H. G. Thorpe, L. J. Kricka, G. Armstrong, *Clin. Chem.* **1989**, *35*, 1441 – 1446; l) G. H. G. Thorpe, I. Bronstein, L. J. Kricka, B. Edwards, J. C. Voyta, *Clin. Chem.* **1989**, *35*, 2319 – 2321; m) I. Bronstein, J. C. Voyta, B. Edwards, *Anal. Biochem.* **1989**, *180*, 95 – 98; n) R. Tizard, R. L. Cate, K. L. Ramachandran, M. Wysk, J. C. Voyta, O. J. Murphy, I. Bronstein, *Proc. Natl. Acad. Sci. USA* **1990**, *87*, 4514 – 4518.

[6] For selected recent reviews on CL applications, see: a) F. J. Lara, D. Airado-Rodriguez, D. Moreno-Gonzalez, J. F. Huertas-Perez, A. M. Garcia-Campana, *Anal. Chim. Acta* **2016**, *913*, 22 – 40; b) Y. X. Liu, X. Y. Huang, J. C. Ren, *Electrophoresis* **2016**, *37*, 2 – 18; c) N. Li, D. Liu, R. Niessner, *Anal. Bioanal. Chem.* **2014**, *406*, 5589 – 5612; d) N. Li, X. Su, Y. Lu, *Analyst* **2015**, *140*, 2916 – 2943; e) M. Iranifam, *TrAC Trends Anal. Chem.* **2014**, *59*, 156 – 183; f) J. F. Huertas-Pérez, D. Moreno-Gonzalez, D. Airado-Rodriguez, F. J. Lara, A. M. Garcia-Campana, *TrAC Trends Anal. Chem.* **2016**, *75*, 35 – 48; g) A. Roda, M. Mirasoli, E. Michelini, M. Di Fusco, M. Zangheri, L. Cevenini, B. Roda, P. Simoni, *Biosens. Bioelectron.* **2016**, *76*, 164 – 179; h) J. Y. Park, L. J. Kricka, *Anal. Bioanal. Chem.* **2014**, *406*, 5631 – 5637; i) Y. Dong, J. Cai, X. You, Y. Chi, *Analyst* **2015**, *140*, 7468 – 7486; j) M. Mirasoli, M. Guardigli, E. Michelini, A. Roda, *J. Pharm. Biomed. Anal.* **2014**, *87*, 36 – 52.

[7] For selected recent reviews on BL applications, see: a) A. Romieu, *Org. Biomol. Chem.* **2015**, *13*, 1294 – 1306; b) S. M. Coleman, A. McGregor, *Future Virol.* **2015**, *10*, 169 – 183; c) T. T. Xu, D. Close, W. Handagama, E. Marr, G. Sayler, S. Ripp, *Front. Oncol.* **2016**, *6*, 150; d) N. Wu, T. Rathnayaka, Y. Kuroda, *Biochimica et Biophysica Acta* **2015**, *1854*, 1392 – 1399; e) G. Y. Lomakina, Y. A. Modestova, N. N. Ugarova, *Biochemistry (Moscow)* **2015**, *80*, 701 – 713; f) M. Hattori, T. Ozawa, *RSC Adv.* **2015**, *5*, 12655 – 12663; g) S. V. Markova, E. S. Vysotski, *Biochemistry (Moscow)* **2015**, *80*, 714 – 732; h) A. Roda, M. Guardigli, E. Michelini, M. Mirasoli, *TrAC Trends Anal. Chem.* **2009**, *29*, 307 – 322; i) E. P. Coutant, Y. L. Janin, *Chem. Eur. J.* **2015**, *21*, 17158 – 17171. See also Refs [6e,j].

[8] For selected recent reviews on ECL applications, see: a) P. Bertoncello, A. J. Stewart, L. Dennany, *Anal. Bioanal. Chem.* **2014**, *406*, 5573 – 5587; b) E. H. Doeven, G. J. Barbante, C. F. Hogan, P. S. Francis, *ChemPlusChem* **2015**, *80*, 456 – 470; c) M. Hesari, Z. Mahdi, *J. Electrochem. Soc.* **2016**, *163*, H3116 – H3131; d) S. E. K. Kirschbaum, A. J. Baeumner, *Anal. Bioanal. Chem.* **2015**, *407*, 3911 – 3926; e) W.-W. Zhao, J. Wang, Y.-C. Zhu, J.-J. Xu, H.-Y. Chen, *Anal. Chem.* **2015**, *87*, 9520 – 9531; f) Z. Liu, W. Qi, G. Xu, *Chem. Soc. Rev.* **2015**, *44*, 3117 – 3142; g) H. Zhou, J. Liu, S. Zhang, *TrAC Trends Anal. Chem.* **2015**, *67*, 56 – 73; h) C. Ding, W. Zhang, W. Wang, Y. Chen, X. Li, *TrAC Trends Anal. Chem.* **2015**, *65*, 137 – 150; i) Y. H. Xu, J. Q. Liu, C. L. Gao, E. K. Wang, *Electrochem. Commun.* **2014**, *48*, 151 – 154; j) S. Zhang, Y. Ding, H. Wei, *Molecules* **2014**, *19*, 11933 – 11987. See also Refs [6e,i,j].

[9] For examples of TCL applications, see: a) M. Gilbert, V. Zakharova, A. Ramenda, C. Jebsen, B. Schulze, C. Wilhelm, *Tetrahedron* **2012**, *68*, 6765 – 6771; b) H. Kong, H. Wang, S. Zhang, X. Zhang, *Analyst* **2011**, *136*, 3643 – 3648; c) Z. Wiener-Megnazi, H. Shiloh, L. Avraham, S. Lahav-Baratz, M. Koifman, A. Z. Reznick, R. Auslender, M. Dirnfeld, *Fertil. Steril.* **2011**, *95*, 979 – 984; d) H. Kong, D. Liu, S. Zhang, X. Zhang, *Anal. Chem.* **2011**, *83*, 1867 – 1870; e) O. Amir, C. Yamin, M. Sagiv, N. Eynon, S. Shnizer, T. Kagan, A. Z. Reznick, M. Sagiv, R. E. Amir, *J. Sports Med. Phys. Fitness* **2009**, *49*, 105 – 111; f) O. Amir, H. Paz, O. Rogowski, M. Barshai, M. Sagiv, S. Shnizer, A. Z. Reznick, R. E. Amir, *Clin. Cardiol.* **2009**, *32*, 199 – 203; g) I. Sukhotnik, V. Brod, M. Lurie, M. A. Rahat, S. Shnizer, N. Lahat, J. G. Mogilner, H. Bitterman, *Crit. Care Med.* **2009**, *37*, 1054 – 1061; h) Z. Wiener-Megnazi, L. Vardi, A. Lissak, S. Shnizer, A. Z. Reznick, D. Ishai, S. Lahav-Baratz, H. Shiloh, M. Koifman, M. Dirnfeld, *Fertil. Steril.* **2004**, *82*, 1171 – 1176; i) S. Shnizer, T. Kagan, A. Lanir, I. Maor, A. A. Reznick, *Luminescence* **2003**, *18*, 90 – 96; j) S. Shnizer, A. Resnik, A. Lanir, V. Piuk, *PCT Int. Appl.* **1999**, WO 9919728A1 19990422; k) J. L. Kiel, J. L. Alls, E. A. Holwitt, L. J. V. Stribling, J. E. Parker, *Bioelectrochem. Bioenerg.* **1998**, *47*, 253 – 257.

[10] a) M. Di Fusco, A. Quintavalla, M. Lombardo, M. Guardigli, M. Mirasoli, C. Trombini, A. Roda, *Anal. Bioanal. Chem.* **2015**, *407*, 1567 – 1576; b) M. Di Fusco, M. Guardigli, M. Lombardo, M. Mirasoli, A. Quintavalla, A. Roda, C. Trombini, *PCT Int. Appl.* **2014**, WO 2014024106A1 20140213; c) M. Di Fusco, A. Quintavalla, C. Trombini, M. Lombardo, A. Roda, M. Guardigli, M. Mirasoli, *J. Org. Chem.* **2013**, *78*, 11238 – 11246; d) A. Roda, M. Di Fusco, A. Quintavalla, M. Guardigli, M. Mirasoli, M. Lombardo, C. Trombini, *Anal. Chem.* **2012**, *84*, 9913 – 9919; see also Ref. [6g].

[11] For 1,2-dioxetanes applied in TCL, see: a) T. Luider, J. C. Hummelen, J. N. Koek, H. Wynberg, Eur. Pat. Appl., **1988**, EP 261719A2 19880330; b) J. C. Hummelen, T. M. Luider, H. Wynberg, *Pure Appl. Chem.* **1987**, *59*, 639 – 650; c) J. C. Hummelen, T. M. Luider, H. Wynberg, *Methods Enzymol.* **1986**, *133*, 531 – 557; d) J. C. Hummelen, H. Wynberg, *PCT Int. Appl.* **1985**, WO 8504958A1 19851107; e) T. M. Luider, J. C. Hummelen, J. N. Koek, D. Oudman, H. Wynberg, in *Luminescence immunoassay and molecular applications*, (Eds.: K. van Dyke, R. van Dyke), CRC Press, Boca Raton, **1990**.

[12] The acridan-containing 1,2-dioxetane **4a** was synthesized for the first time in 1997 and studied as a chemiluminescent (base-induced) label: a) T. Imanishi, Y. Ueda, R. Tainaka, K. Miyashita, *Tetrahedron Lett.* **1997**, *38*, 841 – 844; for other acridan-containing 1,2-dioxetanes, see: b) E. H. White, N. Suzuki, W. H. Hendrickson, *Chem. Lett.* **1979**, *8*, 1491 – 1494; c) N. Suzuki, Y. Kazui, Y. Izawa, *Tetrahedron Lett.* **1982**, *23*, 95 – 96; d) W. Adam, D. Reinhardt, *Liebigs Ann.* **1997**, *7*, 1359 – 1364; e) W. Adam, D. Reinhardt, *J. Chem. Soc. Perkin Trans. 2* **1997**, 1453 – 1463; f) T. Imanishi, Y. Ueda, R. Tainaka, N. Kuni, M. Minagawa, N. Hoshino, K. Miyashita, *Heterocycles* **1998**, *47*, 829 – 838; g) L. F. M. L. Ciscato, F. H. Bartoloni, D. Weiss, R. Beckert, W. J. Baader, *J. Org. Chem.* **2010**, *75*, 6574 – 6580.

[13] For selected reviews on the McMurry reaction, see: a) P. Choudhary, V. Sharma, H. Om, P. Devi, *Am. J. Chem.* **2013**, *3*, 115 – 125; b) T. Takeda, A. Tsubouchi, *Org. React.* **2013**, *82*, 1 – 470; c) M. M. Heravi, Z. Faghihi, *Curr. Org. Chem.* **2012**, *16*, 2097 – 2123; d) G. J. Bodwell, P. R. Nandaluru, *Isr. J. Chem.* **2012**, *52*, 105 – 138; e) M. Iyoda, *Pure Appl. Chem.* **2010**, *82*, 831 – 841; f) T. Takeda, A. Tsubouchi, *Sci. Synth.* **2010**, *47a*, 247 – 325; g) B. Goess, in *Name Reactions for Homologations, McMurry coupling*, (Ed.: J. J. Li), **2009**, pp. 268 – 283; h) M. M. Krayushkin, M. A. Kalik, V. A. Migulin, *Russ. Chem. Rev.* **2009**, *78*, 329 – 336; i) F. T. Ladipo, *Curr. Org. Chem.* **2006**, *10*, 965 – 980; j) M. Ephritikhine, C. Villiers, in *The McMurry coupling and related reactions, Modern Carbonyl Olefination*, (Ed.: T. Takeda), **2004**, pp. 223 – 285; k) A. Fuerstner, in *The McMurry reaction and related transformations, Transition Metals for Organic Synthesis* (Eds.: M. Beller, C. Bolm), 2nd Edition, **2004**, *1*, pp. 449 – 468; l) J. E. McMurry, *Chem. Rev.* **1989**, *89*, 1513 – 1524.

[14] For selected reviews on photooxygenation reaction, see: a) D. Ashen-Garry, M. Selke, *J. Photochem. Photobiol. A* **2014**, *90*, 257 – 274; b) K. K. Banerji, *Org. React. Mech.* **2012**, 79 – 154; c) S. Fukuzumi, K. Ohkubo, in *Photoinduced reactions of radical ions via charge separation, Encyclopedia of Radicals in Chemistry, Biology and Materials*, (Eds.: C. Chatgilialoglu, A. Studer), **2012**, *1*, 365 – 393; d) M. R. Iesce, F. Cermola, in *Photooxygenation [2+2] and [4+2], CRC Handbook of Organic Photochemistry and Photobiology*, (Eds.: A. Griesbeck, M. Oelgemoller, F. Ghetti), 3rd Edition, **2012**, *1*, pp. 727 – 764; e) S. Lacombe, T. Pigot, *Photochemistry* **2010**, *38*, 307 – 329; f) M. Zamadar, A. Greer, in *Singlet oxygen as a reagent in organic synthesis, Handbook of Synthetic Photochemistry*, (Eds.: A. Albini, M. Fagnoni), **2010**, pp. 353 – 386; g) M. Rosaria Iesce, F. Cermola, M. Rubino, *Curr. Org. Chem.* **2007**, *11*, 1053 – 1075; h) E. L. Clennan, A. Pace, *Tetrahedron* **2005**, *61*, 6665 – 6691; i) M. Stratakis, *Curr. Org. Synth.* **2005**, *2*, 281 – 299; j) *Active Oxygen in Chemistry*, (Eds.: C. S. Foote, J. S. Valentine, A. Greenberg, J. F. Liebman), Blackie Academic and Professional, New York, **1995**, Vol. 2; k) C. W. Jefford, *Chem. Soc. Rev.* **1993**, *22*, 59 – 66; l) Z. Jiang, *Res. Chem. Intermed.* **1990**, *14*, 185 – 207; m) L. Lopez, *Top. Curr. Chem.* **1990**, *156*, 117 – 166; n) A. A. Frimer, in *Singlet Oxygen, Volume 2: Reaction Modes and Products*, Part I, CRC Press, Boca Raton, **1985**.

[15] The adamantyl group is widely recognized as a rigid and sterically demanding framework able to significantly stabilize 1,2-dioxetanes: a) F. McCapra, I. Beheshti, A. Burford, R. A. Hann, K. A. Zaklika, *J. Chem. Soc. Chem. Commun.* **1977**, 944 – 946; b) C. Lee, L. A. Singer, *J. Am. Chem. Soc.* **1980**, *102*, 3823 – 3829; c) P. Lechtken, G. Reissenweber, P. Grubmueller, *Tetrahedron Lett.* **1977**, *18*, 2881 – 2884; d) W. Adam, L. A. A. Encarnación, K. Zinner, *Chem. Ber.* **1983**, *116*, 839 – 846; see also Refs. [10c, 12e,g]; for examples of other substituents employed as stabilizing subunits in 1,2-dioxetanes, see: e) M. Matsumoto, H. Suganuma, Y. Katao, H. Mutoh, *J. Chem. Soc. Chem. Commun.* **1995**, 431 – 432; f) L. F. M. L. Ciscato, D. Weiss, R. Beckert, W. J. Baader, *J. Photochem. Photobiol. A* **2011**, *218*, 41 – 47; for a review concerning the medicinal chemistry of adamantane derivatives, see: g) L. Wanka, K. Iqbal, P. R. Schreiner, *Chem. Rev.* **2013**, *113*, 3516 – 3604.

[16] For xanthyl-containing 1,2-dioxetanes, see: a) A. C. Brouwer, J. C. Hummelen, T. M. Luider, F. van Bolhuis, H. Wynberg, *Tetrahedron Lett.* **1988**, *29*, 3137 – 3140; b) A. P. Schaap, M. D. Sandison, R. S. Handley, *Tetrahedron Lett.* **1987**, *28*, 1159 – 1162.

[17] For fluorenyl-containing 1,2-dioxetanes, see: a) W. H. Richardson, S. A. Thomson, *J. Org. Chem.* **1985**, *50*, 1803 – 1810; b) W. Adam, L. A. A. Encarnación, *Chem. Ber.* **1982**, *115*, 2592 – 2605.

[18] We confirmed the nature of the emitting species for methyl-substituted acridan-1,2-dioxetanes (Ref. [10c]) by comparing the TCL spectra of the 1,2-dioxetanes with the fluorescence spectra of the corresponding acridones. In all cases, the TCL spectra closely matched the fluorescence spectra of the corresponding acridones; thus demonstrating that the TCL emission was primarily due to the singlet excited state of acridone. The singlet excited state of 2-adamantanone could also be produced in the TCL process. However, its possible emission could not be detected due to overlap with the fluorescence emission of acridones and the weak intensity. For 2-adamantanone: a) $\lambda_{max} = 425$ nm; G. B. Schuster, N. J. Turro, H.-C. Steinmetzer, A. P. Schaap, G. Faler, W. Adam, J. C. Liu, *J. Am. Chem. Soc.* **1975**, *97*, 7110 – 7118; b) $\phi_F = 0.015$; V. P. Kazakov, A. I. Voloshin, S. S. Ostakhov, N. S. Ableeva, *High Energy Chem.* **1997**, *31*, 109 – 112.

[19] The ability of a *para*-fluorine to decrease the fluorescence quantum yield of the corresponding acridanone was further confirmed by comparing 3-F,6-Me derivative **2l** ($\phi_F = 0.04$) with 3-Me derivative ($\phi_F = 0.21$, reported in ref. [10c]).

[20] The variations of activation energy due to the presence of different substituents are very often paralleled by an analogous change in the pre-exponential coefficient. As a result, the trend in the activation energies often does not reflect the behavior of the kinetic rate constants of the TCL reaction, and thus, the $t_{1/2}$ values.

[21] Although a significant dependence of the CL quantum yield on the substitution pattern was already established for aryl-substituted 1,2-dioxetanes (defined as odd/even rationale), this rationalization refers to chemically triggered dioxetane decomposition, yielding phenolate-like emitting species (strong EDG substitution). In particular, for chemically initiated electron exchange luminescence (CIEEL)-active spiroadamantane 1,2-dioxetanes, such as acetoxynaphthyl spiroadamantyl dioxetanes, it was observed empirically that extended conjugated (*para* substituted) carbonyl chromophores derived from dioxetanes triggered decomposition gave rise to low chemiexcitation efficiencies, whereas cross-conjugated (*meta* substituted) carbonyl compounds showed higher quantum yields. The odd/even rationale was proposed to explain this phenomenon: charge transfer from the donor (phenolate) to the acceptor (carbonyl group) occurs more effectively when the two groups are cross-conjugated (odd number of carbons between the interacting groups), and, presumably, the charge-transfer enhances the excited-state formation and ensures high chemiexcitation efficiency. On the contrary, extended conjugation (even number of carbons between the interacting groups) stabilizes the ground state through dipolar resonance, which disfavors excited-state formation and, consequently, provides low efficiency; see Ref. [5g] and: a) M. Matsumoto, T. Hiroshima, S. Chiba, R. Isobe, N. Watanabe, H. Kobayashi, *Luminescence* **1999**, *14*, 345 – 348; b) Y. Takano, T. Tsunesada, H. Isobe, Y. Yoshioka, K. Yamaguchi, I. Saito, *Bull. Chem. Soc. Jap.* **1999**, *72*, 213 – 225; c) H. Isobe, Y. Takano, M. Okumura, S. Kuramitsu, K. Yamaguchi, *J. Am. Chem. Soc.* **2005**, *127*, 8667 – 8679; d) N. Hoshiya, N. Fukuda, H. Maeda, N. Watanabe, M. Matsumoto, *Tetrahedron* **2006**, *62*, 5808 – 5820; e) L. Yue, Y.-J. Liu, *J. Chem. Theory Comput.* **2013**, *9*, 2300 – 2312; some authors revealed that siloxy- and acetoxy-substituted adamantylideneacridane dioxetanes did not follow the odd/even rationale established for related oxy-substituted benzoates and congeners; see Refs. [11e, 21e].

[22] For chemically or enzymatically triggerable EDG-substituted aryl dioxetanes, on which an EWG was inserted, see: a) I. Bronstein, B. Edwards, A. Sparks, US5538847, **1996**; b) B. P. Giri, WO0014092, **1998**; c) M. Mat-

sumoto, T. Mizuno, N. Watanabe, *Chem. Commun.* **2003**, 482–483; d) B. P. Giri, D. Dagli, WO03054506, **2003**; e) N. Watanabe, T. Mizuno, M. Matsumoto, *Tetrahedron* **2005**, *61*, 9569–9585; f) B. Edwards, R.-R. Juo, A. L. Sparks, US20060079699, **2006**. See also: g) Z. Huang, X. Liang, Y. Chan, *Chin. J. Chem.* **2010**, *9*, 506–511; h) I. Y. Bronstein, B. Edwards, J. C. Voyta, L. J. Kricka, WO8906650, **1989**; for light-triggered 1,2-dioxetanes containing the unsubstituted acridan aromatic system, see Ref. [12g].

[23] The activation parameters for the thermal decomposition of 1,2-dioxetanes **4a** and **4h–t** were determined by a standard isothermal kinetic method, which measured the emission decay kinetics at different temperatures and gave the kinetic constants of the TCL process (see the Supporting Information for details).

[24] For examples of particularly stable 1,2-dioxetanes, see: a) N. Watanabe, M. Kikuchi, Y. Maniwa, H. K. Ijuin, M, Matsumoto, *J. Org. Chem.* **2010**, *75*, 879–884; b) N. Watanabe, Y. Sano, H. Suzuki, M. Tanimura, H. K. Ijuin, M. Matsumoto, *J. Org. Chem.* **2010**, *75*, 5920–5926; c) M. Matsumoto, S. Nasu, M. Takeda, H. Murakami, N. Watanabe, *Chem. Commun.* **2000**, 821–822; d) M. Matsumoto, N. Watanabe, N. C. Kasuga, F. Hamada, K. Tadokoro, *Tetrahedron Lett.* **1997**, *38*, 2863–2866; see also Ref. [18a]; for a theoretical study on the thermal stability of alkyl-substituted 1,2-dioxetanes, see: e) E. L. Bastos, W. J. Baader, *ARKIVOC (Gainesville, FL, U.S.)* **2007**, *8*, 257–272.

[25] The significant increase in the fluorescence quantum yields of acridones containing EDGs could be due to a decrease in the intersystem crossing rate constant, and thus, to a lower efficiency of nonradiative deactivation processes, as reported for aromatic compounds, such as anthracene (N. Nijegorodov, V. Vasilenko, P. Monowe, M. Masale, *Spectrochim. Acta Part A* **2009**, *74*, 188–194).

[26] Concerning the effects of the N-substituent on the fluorescence quantum yield of acridones, see also Ref. [12]. In particular, regarding the effects of the acridan substitution pattern on the fluorescence quantum yields of the emitting species, see Ref. [12e] and references cited therein: in the excitation step of the acridone system, charge is transferred from the donor N atom to the carbonyl group [Eq. (1)].

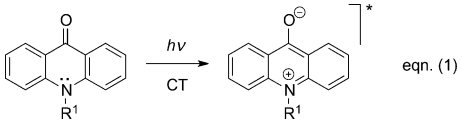

eqn. (1)

The charge-transfer character of the excited acridone chromophore, as expected for a vinylogous amide, is its main electronic characteristic. Thus, it is reasonable that modifications on the nitrogen substituent affect the fluorescence quantum yield much more than the introduction of substituents on the aromatic rings. Furthermore, the position of the aromatic rings substituents perturbs this charge-transfer transition significantly less in acridan-based systems than in benzoate-based systems. For the odd/even rationale established for oxy-substituted benzoates and naphthoates, see: a) A. P. Schaap, R. S. Handley, B. P. Giri, *Tetrahedron Lett.* **1987**, *28*, 935–938; b) A. P. Schaap, T.-S. Chen, R. S. Handley, R. DeSilva, B. P. Giri, *Tetrahedron Lett.* **1987**, *28*, 1155–1158; see also Ref. [21].

[27] This observation is in agreement with the data reported by other authors on *N*-aryl acridan 1,2-dioxetanes (see Ref. [12f]). Considering the possible conformations of *N*-aryl acridan 1,2-dioxetanes, a steric repulsion between the peri-hydrogen atoms of the acridan system and the aryl group might be generated. Therefore, the two rings would not be able to conjugate each other sufficiently and the electronic effects of the aryl group would be largely reduced.

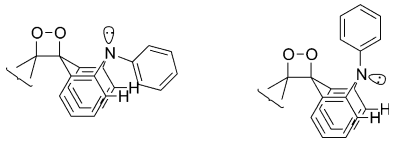

[28] Concerning the photo-oxygenation of sulfur-containing compounds, see: a) E. L. Clennan, in Photooxygenations *of sulfur compounds,* (Eds.: A. Griesbeck, M. Oelgemoller, F. Ghetti), *CRC Handbook of Organic Photochemistry and Photobiology*, 3rd Edition, **2012**, *1*, 789–808; b) E. L. Clennan, S. E. Hightower, *J. Org. Chem.* **2006**, *71*, 1247–1250; c) W. Adam, A. S. Kumar, C. R. Saha-Möller, *Tetrahedron Lett.* **1995**, *36*, 7853–7854; d) F. Cermola, M. R. Iesce, *J. Org. Chem.* **2002**, *67*, 4937–4944. See also Refs [14h, 24a] and cited herein.

[29] a) R. Gompper, *Angew. Chem. Int. Ed. Engl.* **1969**, *8*, 312–327; *Angew. Chem.* **1969**, *81*, 348–363; b) R. W. Hoffmann, *Angew. Chem. Int. Ed. Engl.* **1968**, *7*, 754–765; *Angew. Chem.* **1968**, *80*, 823–835; c) C. S. Foote, A. A. Dzakpasu, J. H.-P. Lin, *Tetrahedron Lett.* **1975**, *16*, 1247–1250; d) P. D. Bartlett, A. P. Schaap, *J. Am. Chem. Soc.* **1970**, *92*, 3223–3225; e) S. Mazur, C. S. Foote, *J. Am. Chem. Soc.* **1970**, *92*, 3225–3226; f) A. P. Schaap, P. D. Bartlett, *J. Am. Chem. Soc.* **1970**, *92*, 6055–6057; see also Ref. [14d] and references cited therein.

[30] For mechanistic studies on photooxygenation of olefins to provide 1,2-dioxetanes, see: a) E. L. Clennan, K. Nagraba, *J. Am. Chem. Soc.* **1988**, *110*, 4312–4318; b) K. Ohkubo, T. Nanjo, S. Fukuzumi, *Org. Lett.* **2005**, *7*, 4265–4268; c) H. Kotani, K. Ohkubo, S. Fukuzumi, *J. Am. Chem. Soc.* **2004**, *126*, 15999–16006; d) Y. Yoshioka, S. Yamada, T. Kawakami, M. Nishino, K. Yamaguchi, I. Saito, *Bull. Chem. Soc. Jpn.* **1996**, *69*, 2683–2699 and cited herein; e) W. Adam, C. R. Saha-Möller, S. B. Schambony, *J. Am. Chem. Soc.* **1999**, *121*, 1834–1838; f) M. Matsumoto, H. Kobayashi, J. Matsubara, N. Watanabe, S. Yamashita, D. Oguma, Y. Kitano, H. Ikawa, *Tetrahedron Lett.* **1996**, *37*, 397–400; g) M. Matsumoto, Y. Kitano, H. Kobayashi, H. Ikawa, *Tetrahedron Lett.* **1996**, *37*, 8191–8194; h) W. Adam, S. G. Bosio, N. J. Turro, *J. Am. Chem. Soc.* **2002**, *124*, 8814–8815; i) T. Poon, J. Sivaguru, R. Franz, S. Jockusch, C. Martinez, I. Washington, W. Adam, Y. Inoue, N. J. Turro, *J. Am. Chem. Soc.* **2004**, *126*, 10498–10499; j) W. Wu, F. An, Z. Geng, R. Zhang, Z. Jiang, *Lett. Org. Chem.* **2013**, *10*, 223–227; k) K. Yamaguchi, S. Yabushita, T. Fueno, K. N. Houk, *J. Am. Chem. Soc.* **1981**, *103*, 5043–5046; l) M. Kojima, M. Nakajoh, C. Matsubara, S. Hashimoto, *J. Chem. Soc. Perkin Trans. 2* **2002**, 1894–1901; see also Ref. [14h] and references cited therein; for a selected example of a mechanistic study on photooxygenation of acenes, see: m) W. Fudickar, T. Linker, *J. Am. Chem. Soc.* **2012**, *134*, 15071–15082.

[31] a) A. Maranzana, G. Ghigo, G. Tonachini, *J. Am. Chem. Soc.* **2000**, *122*, 1414–1423; b) M. Bobrowski, A. Liwo, S. Oldziej, D. Jeziorek, T. Ossowski, *J. Am. Chem. Soc.* **2000**, *122*, 8112–8119; c) F. Sevin, M. L. McKee, *J. Am. Chem. Soc.* **2001**, *123*, 4591–4600.

[32] a) N. Ferré, N. Guihéry, J.-P. Malrieu, *Phys. Chem. Chem. Phys.* **2015**, *17*, 14375–14382; b) K. Yamaguchi, S. Yamanaka, J. Shimada, H. Isobe, T. Saito, M. Shoji, Y. Kitagawa, M. Okumura, *Int. J. Quantum Chem.* **2009**, *109*, 3745–3766.

[33] R. Rajeev, R. B. Sunoj, *J. Org. Chem.* **2012**, *77*, 2474–2485.

[34] a) R. Broa, A. K. Smilde, *Anal. Methods* **2014**, *6*, 2812–2831; b) H. Abdi, L. J. Williams, *WIREs Comp. Stat.* **2010**, *2*, 433–459; c) A. Afifi, S. May, V. A. Clark, in *Practical Multivariate Analysis*, CRC Press, **2011**; d) K. Varmuza, P. Filzmoser, in *Introduction to Multivariate Statistical Analysis in Chemometrics*, CRC Press, **2009**.

[35] For a similar approach, see: L. Eriksson, H. J. M. Verhaar, L. M. Hermens, *Environ. Toxicol. Chem.* **1994**, *13*, 683–691.

[36] a) M. Mousavi-Kamazani, M. Salavati-Niasari, M. Goudarzi, A. Gharehbaii, *J. Inorg. Organomet. Polym. Mater.* **2016**, *26*, 259–263; b) W. Chen, H. Luo, X. Liu, J. W. Foley, X. Song, *Anal. Chem.* **2016**, *88*, 3638–3646; c) V. D. Vandekar, *J. Nat. Prod. Plant Res.* **2015**, *5*, 43–52; d) M. Megala, B. J. M. Rajkumar, *J. Comput. Electron.* **2016**, *15*, 557–568.

[37] a) V. F. Traven, A. V. Manaev, A. Y. Bochkov, T. A. Chibisova, I. V. Ivanov, *Russ. Chem. Bull.* **2012**, *61*, 1342–1362; b) S. Nath, M. Kumbhakar, H. Pal, in *Hydrogen Bonding and Transfer in the Excited State*, (Eds.: K.- L. Han, G.- J. Zhao), **2011**, *1*, pp. 419–431; c) S. Fery-Forgues, C. Fournier-Noel, in *Nanofibers*, (Ed.: A. Kumar), **2010**, pp. 383–404; d) M. A. Musa, J. S. Cooperwood, M. O. F. Khan, *Curr. Med. Chem.* **2008**, *15*, 2664–2679; e) N. Sekar, *Colourage* **2005**, *52*, 71–73; f) J.-P. Goddard, J.-L. Reymond, *Trends Biotechnol.* **2004**, *22*, 363–370; g) B. R. Hirani, M. P. Singh, V. K. Koul, *PharmaChem* **2003**, *2*, 50–52. See also Ref. [22h].

Received: August 5, 2016
Revised: September 7, 2016
Published online on ■■ ▮▮, 0000

FULL PAPER

Substituent Effects

L. A. Andronico, A. Quintavalla, M. Lombardo,* M. Mirasoli, M. Guardigli, C. Trombini, A. Roda*

■■ – ■■

Synthesis of 1,2-Dioxetanes as Thermochemiluminescent Labels for Ultrasensitive Bioassays: Rational Prediction of Olefin Photooxygenation Outcome by Using a Chemometric Approach

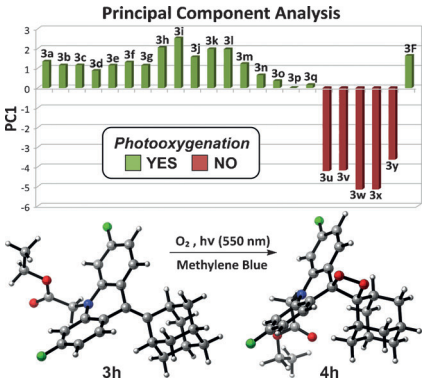

Pick and choose: New high-performance thermochemiluminescent 1,2-dioxetanes for later use in ultrasensitive bioanalytical assays have been synthesized. A chemometric approach enables dioxetane formation to be rationally predicted by defining essential steric and electronic parameters of the olefin precursor (see figure).